

## Transport behavior and critical current densities in MgB<sub>2</sub> wires

**Author/Contributor:**

Pradhan, A; Feng, Y; Zhao, Yong; Koshizuka, N; Zhou, L; Zhang, P; Liu, X; Ji, P; Du, J; Liu, Chengfei

**Publication details:**

Applied Physics Letters

v. 79

pp. 1649-1651

0003-6951 (ISSN)

**Publication Date:**

2001

**Publisher DOI:**

<http://dx.doi.org/10.1063/1.1403278>

**License:**

<https://creativecommons.org/licenses/by-nc-nd/3.0/au/>

Link to license to see what you are allowed to do with this resource.

Downloaded from <http://hdl.handle.net/1959.4/38845> in <https://unsworks.unsw.edu.au> on 2022-07-02

## Transport behavior and critical current densities in MgB<sub>2</sub> wires

A. K. Pradhan,<sup>a)</sup> Y. Feng, Y. Zhao, and N. Koshizuka

*Superconductivity Research Laboratory, ISTEK, 1-10-13 Shinonome, Koto-ku, Tokyo 135-0062, Japan*

L. Zhou, P. X. Zhang, X. H. Liu, P. Ji, S. J. Du, and C. F. Liu

*Northwest Institute of Nonferrous Metal Research, P.O. Box 51, Xi'an 710016, People's Republic of China*

(Received 17 May 2001; accepted for publication 16 July 2001)

We report on the transport and magnetization properties of MgB<sub>2</sub> wires fabricated by a powder-in-tube (PIT) technique. Temperature and magnetic-field-dependent resistivity displays a high conductivity and upper critical field  $H_{c2}$  generally observed in dense samples. The electronic mass anisotropy  $\gamma \approx 1.3 \pm 0.15$  predicts some texturing in the wire. Our data on transition temperature  $T_C$ ,  $H_{c2}$ , and both magnetic and transport critical current density  $J_c$  indicate that MgB<sub>2</sub> can be manufactured in a wire form using a PIT technique and required engineering  $J_c$  can be achieved on further optimization. © 2001 American Institute of Physics.

[DOI: 10.1063/1.1403278]

The recent discovery<sup>1</sup> of superconductivity at 39 K in MgB<sub>2</sub> has generated renewed interest in intermetallic superconductivity. Various physical properties appear to be competitive with well-established A15 conductors used for magnet systems. One of the advantages with MgB<sub>2</sub> is its application at a higher temperature (20–30 K) region, where cryogen free cooling systems can be used in magnetic and nuclear magnetic resonance and other magnet systems. However, unlike conventional superconductors, the fabrication of an actual composite conductor of MgB<sub>2</sub>, that shows uniform properties over a large length of a wire form remains a challenge, mainly due to the ceramic and brittle nature such as high- $T_C$  superconductors, and high pressure synthesis method due to high reactivity with O<sub>2</sub>. This suggests that embedding MgB<sub>2</sub> in a metal sheath by a powder-in-tube (PIT) technique, generally used for fabrication of Ag-sheathed Bi-2223 superconducting tapes, could be a potential solution for manufacturing long length wires for high current applications. The recent reports on fabrication of MgB<sub>2</sub> wires by PIT techniques<sup>2</sup> using either Ag or Cu sheath and MgB<sub>2</sub> strands<sup>3</sup> by directly filling Nb-lined, monel tubes with commercially available MgB<sub>2</sub> powders followed by drawing, rolling into tapes, and sintering<sup>4</sup> were the first steps to put the MgB<sub>2</sub> conductor into applications.

In this letter, we present a very similar technique used for fabrication of Bi-2223/Ag-sheathed tapes by the PIT method to manufacture MgB<sub>2</sub> round wires that are generally demanded for magnet fabrications. We show that these round wires demonstrate remarkably low resistance, moderately high critical current density  $J_c$ , and higher critical fields  $H_{c2}$  without optimization. Our results strongly suggest that high-quality MgB<sub>2</sub> wires can be successfully fabricated at high  $T$ .

MgB<sub>2</sub> composite wires were synthesized by the PIT technique. Stoichiometric composition of high purity Mg and B powders were mixed thoroughly and filled into a Ta tube of 6 mm diameter, and finally inserted into a Cu tube of 10 mm diameter to prevent reaction between Cu and Mg. The

composite tube was swaged and drawn into a wire of 2.1 mm diameter with an intermediate annealing. Finally, the wires were sintered at 900 °C–950 °C for 2–5 h in Ar without high pressure. A similar technique was used to synthesize MgB<sub>2</sub> in a Cu tube without Ta as a buffer (named as MgB<sub>2</sub>-Cu). X-ray diffraction reveals that the MgB<sub>2</sub> phase is present in the core region without any impurities, especially when Ta is used as a buffer layer. The details of the microstructure are reported elsewhere.<sup>5</sup> A small piece of round wire of diameter 2.1 mm and length 3 mm was used for all measurements. High-resolution transport measurements were carried out using standard four-probe ac technique ( $I=1$  mA and  $f=17$  Hz). The transport  $J_c$  was measured using a current reversal dc technique. The magnetization measurements were performed in a superconducting quantum interference device magnetometer.

Figure 1 shows the magnetic field dependence of resistivity of MgB<sub>2</sub>-Ta wire. The midpoint value of normal-state resistivity of the superconducting transition at  $H=0$  is 38.3 K. A similar  $T_C$  value of 38.4 K (with  $\Delta T_C \approx 0.6$  K) was determined from the magnetization measurements as shown in the lower inset of Fig. 1. The dense bulk extracted from the core of the wire shows sharp transition with significantly low transition width (shown as dashed lines in the inset). The normal-state resistivity curve shown in the top inset of Fig. 1 follows roughly usual  $T^2$  temperature dependence over the entire temperature region between 300 K and the onset of  $T_C$  as obtained for dense polycrystalline samples.<sup>6,7</sup> We mention that the resistance due to the metallic sheath is subtracted from the wire resistance and the actual conductor resistance is normalized to the bulk sample extracted from inside the wire. No magnetoresistance was observed from 300 K to  $T_C$  in these wires and this is consistent with previous results on polycrystalline samples,<sup>6,7</sup> but different from the another report.<sup>8</sup> Although no significant broadening of the transition was observed at low fields, a considerable resistive broadening was seen at low temperatures at higher fields, which may be caused by the flux-flow effects at high magnetic fields. This becomes very clear in the Arrhenius plot of resistivity

<sup>a)</sup>Electronic mail: pradhan@istec.or.jp

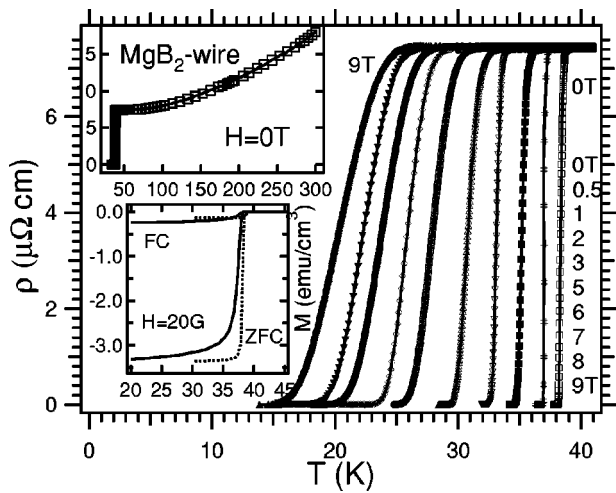


FIG. 1. Temperature-dependent electrical resistivity of  $\text{MgB}_2$ -Ta wire in applied fields  $H=0, 0.5, 1, 2, 3, 5, 6, 7, 8,$  and  $9$  T (right-hand side to left-hand side) for  $H$  parallel to the wire length is shown. The top inset shows the  $T$  dependence of the normal-state resistivity of the same wire for  $H=0$  T. The bottom inset shows the  $T$  dependence of the field-cooled (FC) and zero-FC magnetization of the same wire (solid lines) and the dense bulk (dashed lines) extracted from the core of the wire.

shown in Fig. 2 that shows large slopes at higher field values indicating the thermal activation of the dissipation. However, the role of layered structure in  $\text{MgB}_2$  in causing such dissipation is not known yet. The other option is to consider the impurity effects due to small amount of  $\text{MgO}$  in the interfaces. The resistive behavior of  $\text{MgB}_2$  is significantly similar to that of intermetallic Borocarbide and A15 compounds.

In order to compare the resistive broadening in fields, we plot the upper critical field  $H_{c2}$  as function of reduced temperature ( $T/T_c$ ) in Fig. 3 for  $\text{MgB}_2$ -Ta and  $\text{MgB}_2$ -Cu wires. We mention here that the  $\text{MgB}_2$ -Cu (without Ta as a buffer in between  $\text{MgB}_2$  and Cu) has a  $T_c \sim 38$  K with  $\Delta T_c = 1.2$  K. The slope of the  $H_{c2}$ - $T$  curve yields  $dH_{c2}/dT \approx -0.39$ , which gives  $H_{c2}(0) = 15$  T and  $H_{c2}(4.2 \text{ K}) = 13.2$  T for  $\text{MgB}_2$ -Ta wire. These values are almost half the value of  $H_{c2}(0)$  for  $\text{Nb}_3\text{Sn}$ . In this extrapolation method, we have considered only the linear region above 2 T in the phase diagram, because a small but definite

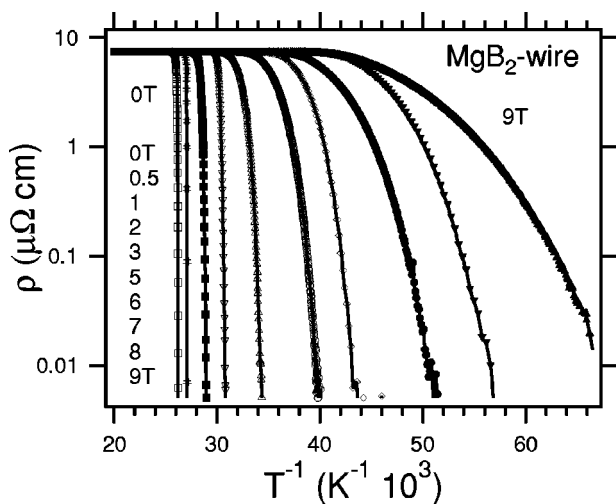


FIG. 2. The Arrhenius plot of resistivity curves at various fields 0 to 9 T (left-hand side to right-hand side) that show large broadening at higher fields is shown.

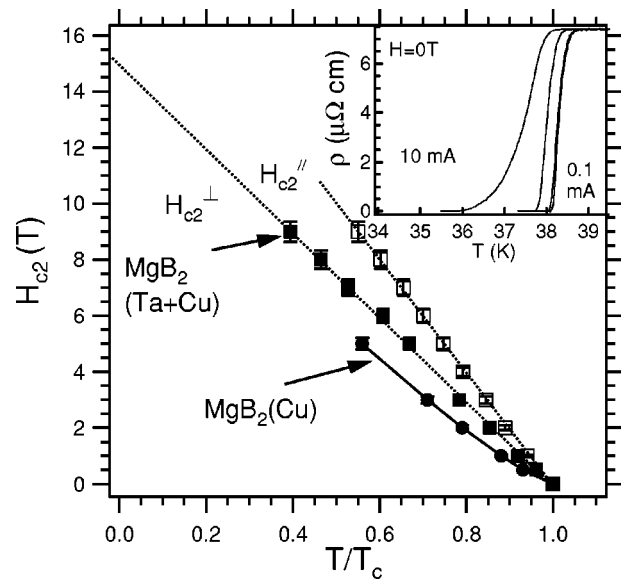


FIG. 3. The upper critical fields  $H_{c2}$  as a function of reduced temperature  $T/T_c$  for  $\text{MgB}_2$ -Ta and  $\text{MgB}_2$ -Cu wires are shown. The inset shows the resistive transition of  $\text{MgB}_2$ -Ta wire for different excitation currents  $I = 0.1, 1, 3,$  and  $10$  mA in zero field.

positive curvature in  $H_{c2}$  was observed in the low-field region in both samples, similar to the borocarbides. Furthermore, it is remarkable to note that the  $T_c$  is found to be very much current-induced due to the self-field effect as shown in the inset of Fig. 3. The pronounced leg feature indicates a large dissipation that is similar to the application of a magnetic field. Hence,  $H_{c2}$  measurements were performed using a current as low as 1 mA. Using the estimation of  $H_{c2}(0) = 15$  T, the coherence length  $\xi_0 = [\phi_0/2\pi H_{c2}(0)]^{0.5}$  is found to be  $\sim 4.5$  nm and consistent with the bulk samples.<sup>9</sup> In order to evaluate the electronic mass anisotropy,  $\gamma = H_{c2}^{\parallel}/H_{c2}^{\perp}$ , we measured both  $H_{c2}^{\perp}$  ( $H$  perpendicular the wire length) and  $H_{c2}^{\parallel}$  ( $H$  parallel to the wire length) in  $\text{MgB}_2$ -Ta for both perpendicular and parallel fields, respectively, and shown in Fig. 3. In contrast to high- $T_c$  layered Bi-2223/Ag multifilamentary tapes,<sup>10</sup>  $\gamma$  is  $\sim 1.3 \pm 0.15$  in  $\text{MgB}_2$ -Ta wire, which is almost half of the value of Bi tapes and less than the  $c$ -axis-oriented thin film,<sup>11</sup> aligned  $\text{MgB}_2$  bulk,<sup>12</sup> and much less than  $\text{Mg}^{11}\text{B}_2$  polycrystalline sample.<sup>13</sup> However, this value does not reflect the actual value of  $\gamma$ , rather indicates that there remain some misoriented grains whose field component is closer to  $H_{c2}^{\perp}$  (or  $H_{c2}^{\parallel}$ ). This shows that the wires are textured to some extent and further optimization can yield highly textured wires for real applications, although enhancing the density of  $\text{MgB}_2$  in the wire core remains the best option to achieve the largest  $J_c$ . However, such a low value of  $\gamma$  can have a serious consequence on reducing transport  $J_c$ .

Figure 4 presents data on both magnetic and transport  $J_c$  of  $\text{MgB}_2$ -Ta wire for magnetic fields applied parallel to the wire length. The dashed lines with symbols are  $J_c$  values extracted from the direct transport measurements of the current-voltage curves at a fixed  $T$  and  $H$ . The solid lines are  $J_c$  values deduced from the magnetization loops using Bean's model. The transport  $J_c$  values (limited to only  $\sim 320$  A/cm<sup>2</sup> due to local heating effects) are consistent with that of magnetization if extrapolated to the low-field region.

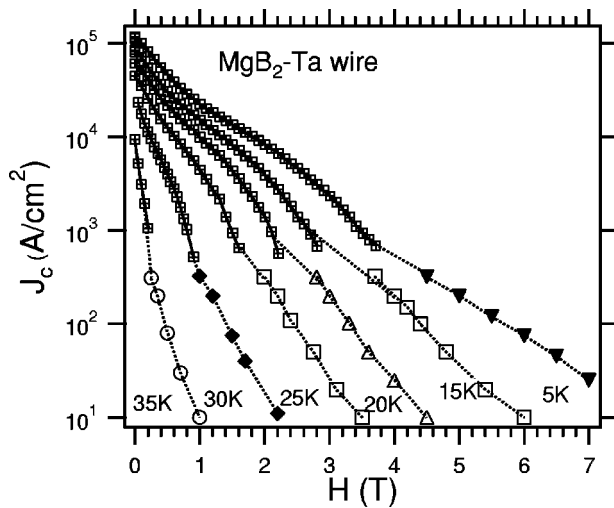


FIG. 4. The critical current density  $J_c$  as a function of applied magnetic field at  $T=5, 15, 20, 25, 30,$  and  $35$  K of  $\text{MgB}_2$ -Ta wire is shown. The symbols with solid lines are the magnetic  $J_c$  of the wire parallel to the wire length. The symbols with dashed lines are the transport  $J_c$ .

Two significant observations are recorded. First, magnetic  $J_c$  decays approximately exponentially above a characteristic plateau in field dependent  $J_c$  curve of the self-field region and may be related to the penetration field, especially at a low temperature. Second, the transport  $J_c$  is higher than the magnetic one at a fixed  $H$  and  $T$  in the high-field region and can be understood in terms of criteria fixed for two independent experiments. However, the overall  $J_c$  values both from transport and magnetization measurements are lower than that of  $\text{MgB}_2$  strands.<sup>3</sup> Moreover, the wires fabricated through *in situ* reaction by a PIT technique have  $\sim 25\%$  lower density than the dense bulk prepared by high pressure synthesis.<sup>2,5</sup> Hence, the effective radius of the wire  $R_{\text{eff}}$  is less than the actual radius  $R$  while calculating using Bean's model defined for magnetic<sup>2</sup>  $J_c$  as  $J_c(H) = 3/2(\Delta M/R)$ . Consequently,  $J_c$  is reduced by 25% of the actual value for the wire. This is mainly due to lower density arising from some scattered porous  $\text{MgB}_2$  matrix in the wire. We note that the extracted dense  $\text{MgB}_2$  bulk from the core the wire produces comparable  $J_c$  values to strands. This suggests many scopes to enhance the flux pinning in the wire by optimizing

the fabrication process. The misorientation and weak connectivity between domains seem to limit  $J_c$  although not as severe as high- $T_c$  superconductors. We mention here that although weak-link phenomenon may not be a reason for low  $J_c$  in  $\text{MgB}_2$  as reported,<sup>14</sup> the link between the domains due to poor density inside the wire remains a primary concern and needs to be addressed further.

In conclusion, our transport and magnetization results on  $\text{MgB}_2$  suggest that embedding  $\text{MgB}_2$  in a copper sheath with Ta as a buffer layer by the standard PIT technique could be a potential solution to attain long length flexible  $\text{MgB}_2$  superconducting wires. Further optimization and preparation sequence of the conductor can result in required properties for applications. At present, the most important requirement for high  $J_c$  is to enhance the density of the  $\text{MgB}_2$  matrix of the wire.

- <sup>1</sup>J. Nagamatsu, N. Nakagawa, T. Muranaka, Y. Zenitani, and J. Akimitsu, *Nature (London)* **410**, 63 (2001).
- <sup>2</sup>B. A. Glowacki, M. Majoros, M. Vickers, J. E. Evetts, Y. Shi, and I. McDougall, *Semicond. Sci. Technol.* **14**, 193 (2001).
- <sup>3</sup>P. C. Canfield, D. K. Finnemore, S. L. Bud'ko, J. E. Ostenson, G. Lapertot, C. E. Cunningham, and C. Petrovic, *Phys. Rev. Lett.* **86**, 2423 (2001).
- <sup>4</sup>M. D. Sumpston, X. Peng, E. Lee, M. Tomsic, and E. W. Collings, *cond-mat/0102441* (2001).
- <sup>5</sup>Y. Feng, Y. Zhao, A. K. Pradhan, L. Zhou, P. X. Zhang, and N. Koshizuka (unpublished).
- <sup>6</sup>Y. Takano, H. Takeya, H. Fujii, H. Kumakura, T. Hatano, K. Tokano, H. Kito, and H. Ihara, *Appl. Phys. Lett.* **78**, 2914 (2001).
- <sup>7</sup>W. N. Kang, C. U. Jung, H. P. Kim, M. Park, S. Y. Lee, H. Kim, E. Choi, K. H. Kim, M. S. Kim, and S. I. Lee, *cond-mat/0102313* (2001).
- <sup>8</sup>D. K. Finnemore, J. E. Ostenson, S. L. Bud'ko, G. Lapertot, and P. C. Canfield, *Phys. Rev. Lett.* **86**, 2420 (2001).
- <sup>9</sup>K.-H. Muller, G. Fuchs, A. Handstein, K. Nenkov, and D. Eckert (unpublished).
- <sup>10</sup>A. K. Pradhan, Y. Feng, Y. Wu, K. Nakao, N. Koshizuka, P. X. Zhang, L. Zhou, and C. S. Li, *J. Appl. Phys.* **89**, 3861 (2001).
- <sup>11</sup>S. Patnaik, L. D. Cooley, and D. C. Larbalestier, *cond-mat/0104562* (2001).
- <sup>12</sup>O. F. de Lima, R. A. Riberio, M. A. Avila, C. A. Cardoso, C. U. Jung, and S.-I. Lee, *cond-mat/0103179* (2001).
- <sup>13</sup>F. Simon, J. Janossy, T. Feher, F. Muranyi, S. Garaj, L. Forro, C. Petrov, S. L. Bud'ko, G. Lapertot, V. G. Kogan, and P. C. Canfield, *cond-mat/0104557* (2001).
- <sup>14</sup>D. C. Larbalestier, M. Rikel, L. D. Cooley, A. A. Polynskii, J. Y. Jiang, S. Patnaik, X. Y. Cai, D. M. Feldmann, A. Gurevich, C. B. Eom, E. E. Hellstrom, R. J. Cava, K. A. Regan, and M. Haas, *Nature (London)* **410**, 186 (2001).